Stem Cell Reports
Article

OPEN ACCESS

Methylation and Transcripts Expression at the Imprinted *GNAS* Locus in Human Embryonic and Induced Pluripotent Stem Cells and Their Derivatives

Virginie Grybek,[1] Laetitia Aubry,[2,3] Stéphanie Maupetit-Méhouas,[1,8] Catherine Le Stunff,[1] Cécile Denis,[4] Mathilde Girard,[4] Agnès Linglart,[1,5,6] and Caroline Silve[1,6,7,*]

[1]INSERM U986, Hôpital Bicêtre, Le Kremlin Bicêtre 94276, France
[2]UEVE UMR 861, I-Stem, AFM, Evry 91030, France
[3]INSERM UMR 861, I-Stem, AFM, Evry 91030, France
[4]CECS, I-Stem, AFM, Institute for Stem Cell Therapy and Exploration of Monogenic Diseases, Evry 91030, France
[5]Service d'Endocrinologie Pédiatrique, Hôpital Bicêtre-AP-HP, Le Kremlin Bicêtre 94276, France
[6]Centre de Référence des Maladies Rares du Métabolisme Phospho-Calcique Hôpital Bicêtre, Le Kremlin Bicêtre 94276, France
[7]Laboratoire de Biochimie Hormonale et Génétique, Hôpital Bichat Claude Bernard-AP-HP, Paris 75018, France
[8]Present address: Laboratoire GReD, P. Arnaud Team, CNRS 6293, Clermont Université, INSERM U1103, Faculté de Médecine, Clermont-Ferrand Cedex 63001, France
*Correspondence: caroline.silve@inserm.fr
http://dx.doi.org/10.1016/j.stemcr.2014.07.002

SUMMARY

Data from the literature indicate that genomic imprint marks are disturbed in human pluripotent stem cells (PSCs). *GNAS* is an imprinted locus that produces one biallelic (*Gsα*) and four monoallelic (*NESP55*, *GNAS-AS1*, *XLsα*, and *A/B*) transcripts due to differential methylation of their promoters (DMR). To document imprinting at the *GNAS* locus in PSCs, we studied *GNAS* locus DMR methylation and transcript (*NESP55*, *XLsα*, and *A/B*) expression in human embryonic stem cells (hESCs) and human induced pluripotent stem cells (hiPSCs) derived from two human fibroblasts and their progenies. Results showed that (1) methylation at the *GNAS* locus DMRs is DMR and cell line specific, (2) changes in allelic transcript expression can be independent of a change in allele-specific DNA methylation, and (3) interestingly, methylation at A/B DMR is correlated with *A/B* transcript expression. These results indicate that these models are valuable to study the mechanisms controlling *GNAS* methylation, factors involved in transcript expression, and possibly mechanisms involved in the pathophysiology of pseudohypoparathyroidism type 1B.

INTRODUCTION

Human pluripotent stem cells (PSCs) provide invaluable models to study development, human diseases, and regenerative therapies. They can be derived from blastocysts (human embryonic stem cells [hESCs]) or directly reprogrammed from somatic cells (human induced pluripotent stem cells [hiPSCs]) (MacDonald and Mann 2014; Sabour and Schöler 2012; Tobin and Kim 2012). They share the unique property of self-renewal and are both expected to express the paternal and maternal imprints established during gametogenesis and maintained following fertilization. Imprinting maintenance and erasure are essential processes required for the mammalian development (Girardot et al., 2013; Laird 2013; Reik et al., 2001). However, hESCs are derived from a period in mammalian development characterized by global epigenetic remodeling, raising the possibility that the genomic imprint marks may be disturbed in these cells, whereas it is argued that nuclear reprogramming of hiPSCs could erase them (Li and Sasaki 2011; Takikawa et al., 2013). Therefore, it is important to assess if methylation marks at imprinted loci are stable or subject to variation upon derivation technique and subsequent culture.

GNAS is an imprinted locus that produces several transcripts comprising *Gsα*, the alpha-stimulatory subunit of the G protein; *XLsα*; *A/B* (also referred as *1A*); *NESP55*; and the antisense transcript *GNAS-AS1*. Due to differential methylation of their promoters (DMR), *XLsα*, *A/B*, *NESP55*, and *GNAS-AS1* originate from one parental allele only. *XLsα*, *A/B*, and *GNAS-AS1* are transcribed from the paternal allele; *NESP55* is transcribed from the maternal allele only. The promoter of *Gsα* is not differentially methylated, and therefore, *Gsα* expression arises from both alleles in most tissues (Figure 1). In a few specific tissues, however, including the renal proximal tubule, the thyroid, the pituitary, and the gonads, *Gsα* is expressed from the maternal allele only (Bastepe and Jüppner 2005; Hayward et al., 1998a, b; Levine 2012; Linglart et al., 2013; Mantovani et al., 2002; Plagge and Kelsey 2006; Weinstein et al., 2001). Maternally and paternally inherited loss of function of Gsα cause pseudohypoparathyroidism (PHP) type 1A (OMIM 103580) and pseudoPHP, respectively (or progressive osseous heteroplasia). Epigenetic changes at one or several of the promoters of the *GNAS* locus cause PHP type 1B (PHP1B) (OMIM 603233). All patients affected with PHP1B share a loss of methylation (LOM) at the maternal promoter of *A/B*, which results in suppressed *Gsα* transcription in imprinted tissues. LOM can be restricted to the A/B promoter of *GNAS*, as found in most familial forms of PHP1B (autosomic dominant PHP1B

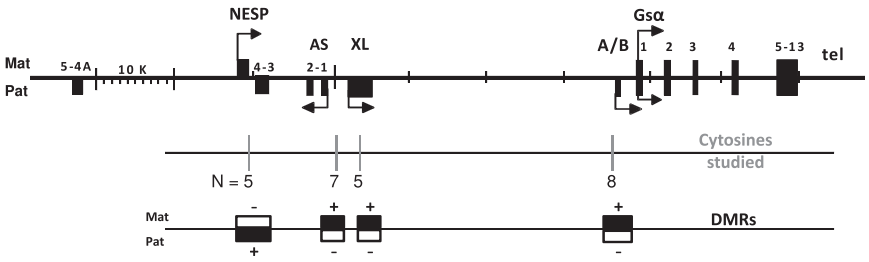

Figure 1. Schematic Drawing of the *GNAS* Locus

The *GNAS* locus is scaled, based on HG19. The four differentially methylated regions studied in this report are represented below the genomic line by black boxes (+ or methylated) or white boxes (− or unmethylated) on the paternal (Pat) or maternal (Mat) allele. Exons are indicated as black rectangles and allelic origin of transcription as broken arrows on the Pat or Mat allele. Positions and number of analyzed cytosines regarding methylation analysis are also indicated.

[AD-PHP1B]). Alternatively, A/B DMR LOM can be associated with methylation changes at other DMRs of *GNAS* on the maternal allele, as found in rare families carrying deletions removing an imprinting control element close to the AS and NESP DMRs, or most frequently in patients with sporadic PHP1B (80%–85% of PHP1B patients) (Bastepe and Jüppner 2005; Hayward et al., 1998a, b; Levine 2012; Linglart et al., 2013; Mantovani et al., 2002; Plagge and Kelsey 2006; Weinstein et al., 2001).

The molecular mechanisms controlling the establishment of imprinting at the *GNAS* cluster and leading to the methylation defects in PHP1B are mostly unknown, in part because of a paucity of suitable animal models and lack of accessible Gsα-imprinted human tissues. During the murine embryonic development, the differential methylation of exon 1A (A/B in humans) and Nespas/Gnasxl (AS and XL in humans) DMRs is established during the oogenesis (germline DMRs) whereas the differential methylation of Nesp DMR occurs postfertilization (somatic DMR), with a key role played by *Nesp* transcription in establishing the specific-allele methylation at the *Gnas* locus (Chotalia et al., 2009; Coombes et al., 2003; Liu et al., 2000). A recent study analyzing a large number of human fetal gonads from gestational weeks 6.5–22 suggested that epigenetic reprogramming in human primordial germ cells (hPGCs) probably involves, as observed in mice but with a different timing, two distinct periods: an early wave of genome-wide demethylation before 7 weeks of gestation and a later wave of imprint erasure and changes in chromatin modifications after 9 weeks of gestation (Gkountela et al., 2013; Laird 2013). Studies in hESCs and hPGCs indicated that allelic silencing of *A/B* is established during the gametogenesis (Frost et al., 2011) and that of *XLsα* already established at 5 weeks postfertilization (supporting the gametic specific-allele methylation of both A/B and XL DMRs as observed in the mice) (Crane et al., 2009). The complete allelic silencing of the *NESP55* transcript occurs during implantation 5–11 weeks after fertilization (Crane et al., 2009; Rugg-Gunn et al., 2005a, b), in agreement with a somatic DMR. Tissue-specific silencing of paternal *Gsα* most likely takes place after 11 weeks postfertilization and after tissue differentiation (Turan et al., 2014; Zheng et al., 2001). A genome-wide DNA methylation revealed the maintenance of *GNAS* methylation in hiPSCs with culture, although hypermethylation and hypomethylation were also observed (Nazor et al., 2012).

In an effort to document imprinting at the *GNAS* locus and contribute to the development of models allowing its dynamic study and tissue-specific silencing of paternal *Gsα* in (patho)physiological conditions in humans, we studied methylation at the four *GNAS* DMRs in hESCs and hiPSCs and their progenies. We also examined the expression of four *GNAS* transcripts (*Gsα*, *A/B*, *XLsα*, and *NESP55*) in hiPSCs and derivatives.

RESULTS

Characterization of Cell Lines

Somatic, pluripotent stem, and differentiated cells studied are presented in Table 1. Characterization of all hiPSC and ESC lines revealed a normal karyotype (including the VUBO1P91 cell line, studied at a high passage), expression of pluripotency markers, and expression of markers of the three germ layers upon in vitro embryoid bodies differentiation as illustrated in Figure 2 for hiPSC i90c17 line. In addition, all neural stem cells (NSCs) and mesenchymal stem cells (MSCs) expressed, respectively, the neural markers Nestin and Sox2 and the mesenchymal markers CD29, CD44, CD73, and CD166, as illustrated in Figure 2 for NSCs and MSCs derived from hiPSC i90c17 line.

Comparison of overall transcript levels between the various cell types by quantitative real-time PCR (qRT-PCR) indicated similar patterns of expression. When comparing fibroblasts and derived hiPSCs, an increase in all transcripts expression was observed. When comparing PSCs (hESCs and hiPSCs) in both NSC and MSC progenies, a decrease in *NESP55*, *XLsα*, and *A/B* transcripts expression was present, whereas *Gsα* transcript expression increased upon differentiation (Figure S1 available online).

Table 1. Somatic, Pluripotent Stem, and Differentiated Cells Studied

Somatic Cells	PSCs	Differentiated Cells (Progenies)	Allelic Expression	Overall Transcript Levels
h fibroblasts IMR90 (XX)	hiPSC i90c01 (retrovirus)	MSC/NSC	Fb/hiPSC/MSC	Fb/hiPSC/MSC/NCS
	hiPSC i90c17 (episome)	MSC/NSC	Fb/hiPSC/MSC/NSC	Fb/hiPSC/MSC/NSC
h fibroblasts GM04603 (XY)	hiPSC 4603c27 (retrovirus)	MSC/NSC	Fb/hiPSC/MSC/NSC	Fb/hiPSC/MSC/NSC
	hiPSC 4603 polyF (retrovirus)		Fb/hiPSC	Fb/hiPSC
	hESC VUB01 (XY)	NSC	0	Fb/hESC/NSC
	hESC W09 (XX)	MSC	0	Fb/hESC/MSC
	hESC RC9 (XY)		0	
	hESC SA01 (XY)	NSC	0	Fb/hESC/NSC

For each cell line, whether overall (shown in Figure S1) and allelic (shown in Figure 5) transcript expressions were analyzed is indicated. Methylation at the *GNAS* DMRs was studied for all cells except hiPSC i90_c01 NSC. Fb, fibroblast; h, human; hESC, human embryonic stem cells; hiPSC, human induced pluripotent stem cells; MSC, mesenchymal stem cells; NSC, neuronal stem cells. "0" indicates homozygosity at the DNA level (all hESC). Only heterozygous cells at the DNA level were analyzed for transcript expression. Overall and allelic expressions were analyzed as described in the Experimental Procedures section.

Methylation at the *GNAS* Locus DMRs

In order to study the maintenance of imprinting at the *GNAS* locus, we quantified and compared methylation at the *GNAS* locus DMRs in eight PSCs (four hESCs and four hiPSCs), their progenies (four MSCs and four NSCs), and the two parental fibroblast cell lines and controls.

hESCs/hiPSCs

We first compared methylation indices at the *GNAS* DMRs measured in the four hESCs and four hiPSCs (Figures 3 and S2). Results showed that percent of methylation at each DMR was not significantly different when comparing hESCs and hiPSCs (NESP: hESCs: 43.7% ± 2.76%, hiPSC: 46.8% ± 3.07%; AS: hESC: 36.9% ± 16.42%, hiPSC: 34.3% ± 17.33%; XL: hESC: 49.0% ± 7.27%, hiPSC: 48.5% ± 4.6%; A/B: hESC: 38.6% ± 12.57%, hiPSC: 35.7% ± 13.73%; $p > 0.05$ for each DMR; mean ± SD; n = 4 for all groups).

PSCs/Controls

Because methylation at the *GNAS* DMRs was not significantly different in hESCs and hiPSCs, we then compared methylation at each *GNAS* DMRs comparing all PSCs (hESCs + hiPSCs) to that measured in blood DNA from 20 controls (Figure 3). Results indicated that percent of methylation at the NESP and XL DMRs was not significantly different when comparing PSCs and controls (PSCs, NESP: 45.2% ± 3.15%, XL: 48.8% ± 5.63%; controls, NESP: 49.3% ± 2.34%, XL: 47.28% ± 3.44%; $p > 0.05$; Figure 3). In contrast, percent of methylation at the AS and A/B DMRs was significantly lower when comparing PSCs and controls (PSCs, AS: 35.6% ± 15.69%, A/B: 37.2% ± 12.29%; controls, AS: 49.5% ± 1.39%, A/B: 51.9% ± 2.07%; $p < 0.01$ and 0.001, respectively, for AS and A/B; mean ± SD; n = 8 for PSCs and 20 for controls).

Percent of methylation for each DMR in the two parental fibroblast cell lines was within the range of values obtained in genomic DNA from controls (Figure 3).

We also compared the dispersion of *GNAS* DMR methylation between groups. The methylation scatter at the AS and A/B DMRs, but not at the NESP and XL DMRs, was significantly higher at the AS and A/B DMRs in PSCs compared to that in controls (PSCs, AS: 12.5% ± 8.66%, A/B: 8.5% ± 8.80%; controls, AS: 1.2% ± 0.69%, A/B: 1.6% ± 1.28%; $p < 0.001$ and $p < 0.01$, respectively, for AS and A/B; mean ± SD; data not shown). These results further support that the methylation at the AS and A/B DMRs is less stringent than that at the NESP and XL DMRs in PSCs and compared to controls.

PSCs/Progenies

PSCs were differentiated in four MSCs (three from hiPSCs and one from hESCs) and four NSCs (two from hiPSCs and two from hESCs). When comparing NSC progenies to appropriate PSCs, an increase in percent of methylation was observed in 2/4, 4/4, and 2/4, respectively, at the NESP, AS, and A/B DMRs and a decrease in 1/4 and 2/4, respectively, at the XL and A/B DMRs (Figures 4 and S3). Changes in percent of methylation were observed for NSC obtained from both hESCs and hiPSCs (Figures 4 and S3). When comparing MSC progenies to appropriate PSCs, methylation at NESP, XL, and A/B DMRs were similar. As in NSC, an increase in percent of methylation at AS DMR was also observed in MSC compared to appropriate PSCs. Thus, at the AS DMR, percent of methylation was significantly higher in MSC and NSC progenies compared to PSCs (Figure 4) (progenies: 66.1% ± 20.63%; controls: 39.0% ± 13.42%; $p < 0.001$; mean ± SD; n = 6 for progenies and PSCs).

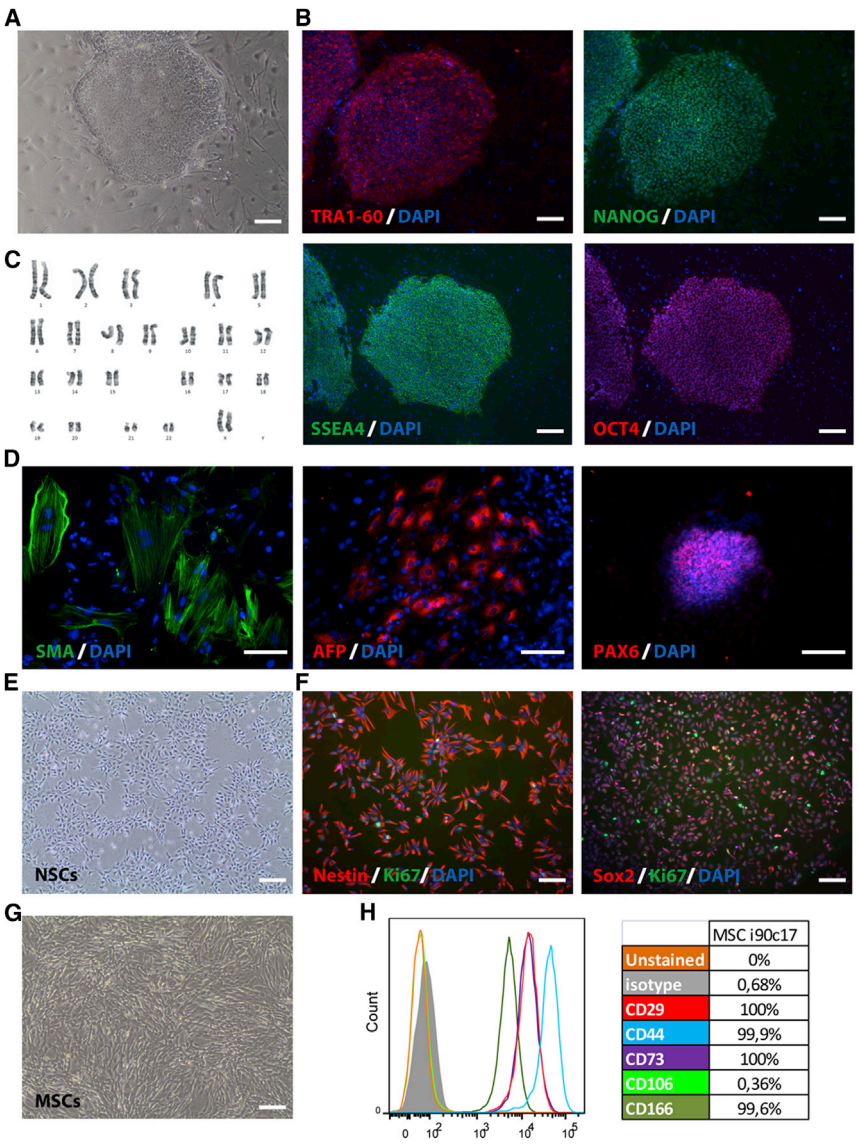

Figure 2. Characterization of i90c17 Human Induced Pluripotent Stem Cells and Neural Stem Cells and Mesenchymal Stem Cells Derived from i90c17 hiPSC Line

(A) Phase-contrast image of an i90c17 hiPSCs colony on feeder cell.

(B) Immunostaining showing the expression of the pluripotency markers TRA1-60, NANOG, SSEA4, and OCT4 in i90c17 hiPSC line.

(C) G-banding chromosome analysis of i90c17 hiPSCs showing a normal karyotype (46, XX).

(D) In vitro embryoid body formation from i90c17 hiPSCs showed three germ layer differentiation as illustrated by the presence of endodermal AFP+ cells, neuroectodermal PAX6+ cells, and mesodermal SMA+ cells.

(E) Phase-contrast image of hiPSCs i90c17-derived NSCs.

(F) Immunostaining showing the expression of the neural (Nestin and Sox2) and proliferating (Ki67) markers in hiPSCs i90c17-derived NSCs.

(G) Phase-contrast image of i90c17 hiPSCs-derived MSCs.

(H) Flow cytometry analysis of CD29, CD44, CD73, CD106, and CD166 expression in i90c17 hiPSCs-derived MSCs.

hiPSC, human pluripotent stem cell; MSC, mesenchymal stem cell; NSC, neural stem cell. The scale bars represent 200 μm. See also Figure S1.

Allelic Expression in Fibroblasts and Derived hiPSCs and Progenies

We determined that the two parental fibroblasts were heterozygous for the polymorphism rs7121 T/C in exon 5 (*GNAS* T393C) at the genomic DNA level (%T: 49.7% and 48.2% in IMR90 and GM04603, respectively) and that their derivative cells maintained heterozygosis (data not shown), thereby allowing analysis of *GNAS* transcript allelic expression as a function of reprogramming and differentiation. All hESCs were homozygous for rs7121 (data not shown).

NESP55 transcripts were detected only in 3/4 hiPSCs and showed monoallelic expression (%T expression: 100% and 98% in hiPSCs 4603_c27 and polyF, respectively; %C: 94% in hiPSC i90_c01) (Figures 5, S4, and S5); they were not detected in fibroblasts or in progenies. As indicated in the Experimental Procedures section, given that *NESP55* is essentially maternally expressed, transcript expression is thus expressed as "percent maternal allele ratio."

As expected, expression of *Gsα* transcripts was biallelic in the two parental fibroblasts (58.40% and 56.60% maternal allele ratio in fibroblasts i90 and i4603, respectively) (Figures 5 and S3). *Gsα* remained biallelic after reprogramming in hiPSCs and differentiation in progenies (maternal allele ratio: 47.4% ± 5.8% and 54.8% ± 2.71%, respectively, in hiPSCs and hiPSC progenies; mean ± SD; n = 6) (Figures 5 and S5).

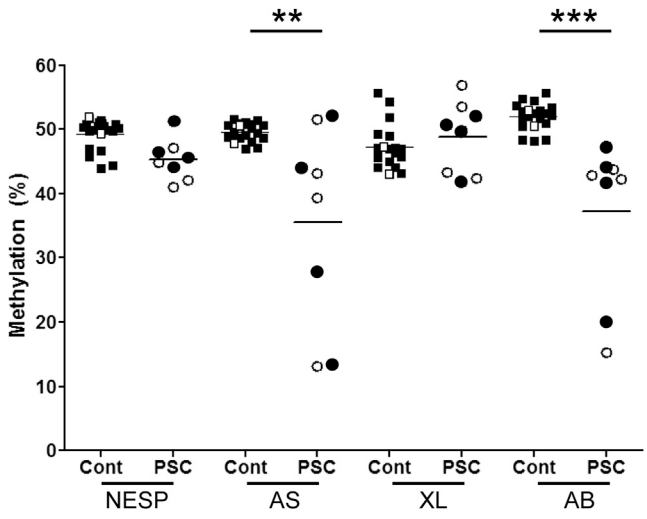

Figure 3. Methylation Quantification at the DMRs of *GNAS* in PSCs Compared to Parental Fibroblasts

Methylation at each of the four DMRs was similar comparing hESCs (○) and hiPSCs (●) and for NESP and XL DMRs, similar to 20 control subjects (■) and parental fibroblasts (□). Methylation at the AS and A/B DMRs was significantly lower when comparing PSCs and controls (**p < 0.01; ***p < 0.001). Cell cultures, quantification of methylation, and statistical analysis were performed as described in the Experimental Procedures section. See also Figure S2.

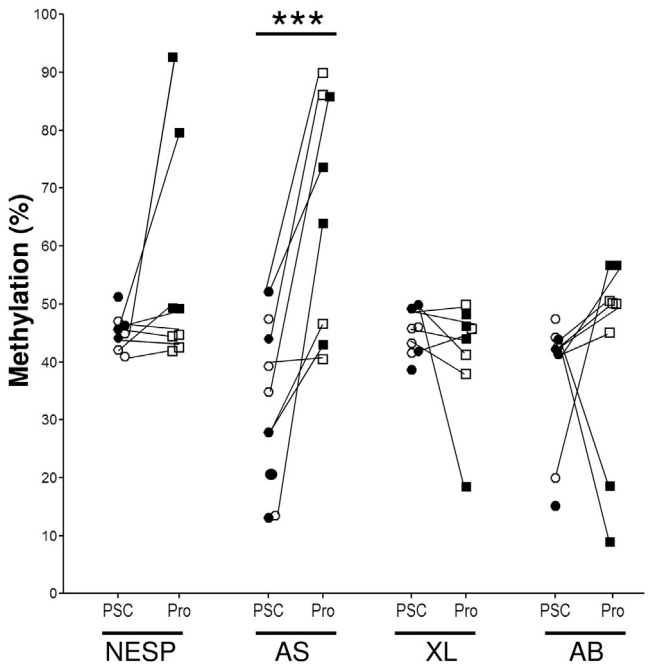

Figure 4. Methylation Quantification at the Four DMRs of *GNAS* in PSCs Compared to Progenies

Methylation at the *GNAS* locus is affected both as a function of cell type (NSC ■ versus MSC □) and DMRs: changes in percent of methylation were observed at the NESP, XL, and A/B DMRs when comparing NSC, but not MSC, to appropriate PSCs (hiPSCs: ●; hESCs: ○); methylation at the AS DMR increases in both MSC and NSC and was significantly higher than that in PSCs (***p < 0.001). Cell cultures, quantification of methylation, and statistical analysis were performed as described in the Experimental Procedures section. See also Figure S3.

Expression of *XLsα* transcripts was monoallelic in the two parental fibroblasts and showed, as expected, paternal expression (3.8% and 3.6% maternal expression in i90 and in 4603, respectively) (Figures 5 and S5). Surprisingly, after reprogramming in hiPSCs, *XLsα* was biallelic (maternal allele ratio 43.1% ± 3.86%; mean ± SD; n = 4) in all cells. In MSC- and NSC-differentiated cells, *XLsα* expression was again monoallelic (maternal allele ratio 3.9% ± 4.61%; mean ± SD; n = 5), except in one NCS line, in which it stayed biallelic.

As observed for *XLsα* transcripts, expression of *A/B* transcripts was also monoallelic in the two parental fibroblasts with paternal expression (5.2% and 0% maternal expression in i90 and in 4603, respectively). Monoallelic expression of *A/B* transcript was conserved in the two hiPSC i90 clones (maternal allele ratio 0% and 0.8%), but not in the hiPSC 4603 clones, in which expression of *A/B* transcripts increased and presented partial allelic and biallelic (maternal allele ratio 21.3% and 41.2%) (Figures 5 and S3). In MSC- and NSC-differentiated cells, *A/B* expression was monoallelic and paternally expressed (maternal allele ratio 4.26% ± 3.89%; mean ± SD; n = 5), except in one NCS line, in which it increased and became biallelic (maternal allele ratio 59.1%). The rs7121 polymorphism is not present in *GNAS-AS1* cDNA, therefore precluding *GNAS-AS1* allelic expression.

Correlation between DMR Methylation and Allelic Expression

In "normal" conditions, XL and A/B promoters are differentially methylated (i.e., methylated on the maternal allele) and *XLsα* and *A/B* transcript expression is described as monoallelic (expression of 90%–100% of a major paternal allele). Changes of methylation are usually associated with changes in parental transcript expression. In order to determine if *XLsα* and *A/B* transcript expression was correlated to *GNAS* DMR methylation, we correlated allelic expression to methylation at the XL and A/B *GNAS* DMRs in fibroblasts and derivatives. We found that the allelic expression of *A/B* transcripts, but not that of *XLsα* with XL DMR, was correlated with A/B DMR methylation (Figures 6A and 6B): the ratio of *A/B* maternal allele expression decreased when methylation at A/B DMR increased (Pearson r: 0.8974, p = 0.001 and Pearson r: 0.4425, p = ns for A/B and XL, respectively). *Gsα* allelic expression was not correlated with percent methylation of A/B DMR or with *A/B* transcript expression (data not shown). Allelic

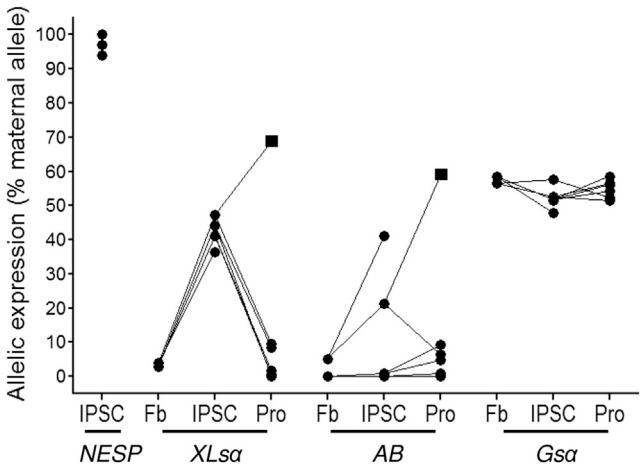

Figure 5. Allelic Transcript Expression in Parental Fibroblasts, hiPSCs, and Progenies

NESP55 transcript, detected in three hiPSC clones, was monoallelic. *XLsα* expression was monoallelic in the two parental fibroblast (Fb) lines, biallelic in the four hiPSC clones, and returned to monoallelic expression in progenies except one (NSC, ■). *A/B* expression was monoallelic in the two parental fibroblast lines, in 2/4 hiPSC clones, and in progenies (Freson et al., 2008) except one (NSC, ■). *Gsα* was biallelic in the two parental fibroblast lines, the four hiPSC clones, and progenies. Cell cultures and allelic transcript expression were performed as described in the Experimental Procedures section. Expression for *GNAS* transcripts are expressed as percent maternal allele ratio, based on the allele expression of the maternally expressed *NESP55* transcript (see Experimental Procedures for details). Biallelic expression was defined for maternal allele ratio comprised between 40% and 60% and monoallelic expression for maternal allele ratio comprised between 90% and 100% and 0% and 10%. See also Figures S4 and S5.

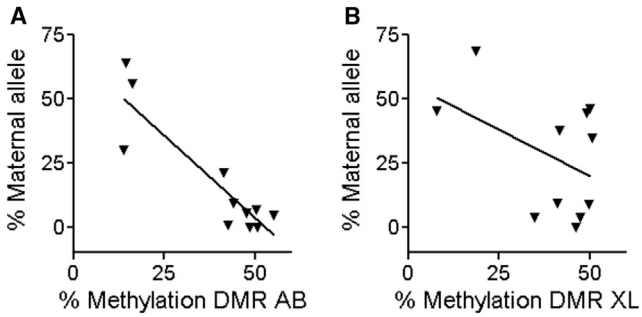

Figure 6. Correlation between Methylation and Allelic Expression for *A/B* and *XLsα*

The allelic expression of *A/B* transcript (A), but not that of *XLsα* (B), correlates with the methylation at their DMRs (Pearson r: A/B: 0.8974, p = 0.001; XL: 0.4425, p = not significant). Cell cultures, quantification of DMR methylation, and analysis of allelic transcript expression were performed as described in the Experimental Procedures section. *GNAS* transcripts are expressed as percent maternal allele ratio, based on the allele of the maternally expressed *NESP55* transcript (see Experimental Procedures for details).

transcript expression analysis was not available for *GNAS-AS1* and was available in only three samples for *NESP55*, precluding any correlation (data not shown).

DISCUSSION

To assess if methylation marks at the *GNAS* locus were maintained in hESCs and hiPSCs or subjected to variation upon derivation technique and subsequent culture, we quantified and compared methylation at the *GNAS* locus in hESCs and hiPSCs (four cell lines each). Our results showed that methylation at the four DMRs was similar in hESCs and hiPSCs. These results are consistent with a whole-genome single-base resolution DNA methylome study by Lister et al. (2011) reporting globally similar methylation comparing hESC and hiPSC methylomes. In addition, we found that methylation at the paternally imprinted NESP (maternal expression of the transcript) and maternally imprinted XL (paternal expression of the transcript) DMRs was maintained in all PSCs (hESCs and hiPSCs) and similar to that in controls and parental fibroblasts, in contrast to the two maternally imprinted AS and A/B DMRs.

Two main conclusions can be drawn from these observations. First, previous studies have indicated that epigenetic instability is a rare occurrence in hESCs but, in contrast, that the differential methylation that marks imprinted loci could be erased during nuclear reprogramming of somatic cells (Frost et al., 2011). Analysis of germline methylation imprints in human PSCs has revealed some instability and this independently of the parental origin of the imprint (Lund et al., 2012; Nazor et al., 2012; Rugg-Gunn et al., 2007; Takikawa et al., 2013; Tobin and Kim 2012). In this regard, aberrant DNA methylation at the maternally imprinted *H19* and paternally imprinted *KCNQOT1* genes in iPSCs has been reported (Lister et al., 2011). Our results indicate that the control of *GNAS* genomic methylation imprinting stability does not vary specifically as function of the PSC type (hESCs versus hiPSCs) and is independent of the reprogramming procedure. This is further supported by the similar methylation pattern observed for two clones obtained from the same parental fibroblast either by retroviral or episomal reprogramming methods. Second, our results indicate that the control of methylation at the NESP and XL DMRs (paternally and maternally imprinted, respectively) is more stringent than that at AS and A/B DMR (both maternally imprinted). NESP DMR methylation analyzed in two studies was reported differentially methylated in the majority of hESC lines with exceptional loss or gain of methylation (Frost et al., 2011; Huntriss

et al., 2011). Methylation of XL DMR reported in only two human in vitro fertilization blastocysts was variable (4.8% and 77.1%) (Huntriss et al., 2011). Our results further document and enrich these observations. In all cases of DMR methylation instability, we observed demethylation and not hypermethylation, indicating that whatever the underlying mechanism, AS and A/B are prone to demethylation during PSC derivation or maintenance. Why the control of methylation at the AS and A/B DMRs is less stringent than that at the NESP and XL DMRs in PSCs is not explained. Methylation at the A/B DMR was low in the polyclonal iPSC04603_polyF cell line and normal in the monoclonal iPSC04603_c27 line, both derived from the same parental fibroblasts, raising the possibility that clonality may affect methylation results.

An important aspect of PSC research is their theoretical ability to be differentiated into any cell type, including cells expressing tissue-specific silencing of paternal *Gsα*, as described for Gsα. However, for such studies, it is critical to fully control the differentiation of these PSCs into specific cellular types of interest. Thus, our next step was to study methylation marks upon differentiation of PSCs. Our results indicate that methylation at the *GNAS* locus is affected both as a function of cell type (NSC versus MSC) and DMRs. Indeed, methylation changes at the NESP and A/B DMRs were observed only upon differentiation into NSC, not MSC. In addition, we observed an increase in AS methylation in all progenies (NSC and MSC), reaching hypermethylation levels in 4/8. Few reports, and none for the *GNAS* locus to our knowledge, have addressed the issue of DMR methylation upon "re"differentiation of PSCs into progenies in human cells. The pattern associating gain of methylation at NESP and loss of methylation at A/B and/or XL DMRs of *GNAS* is reminiscent to that of patients affected with sporadic PHP1B. Whereas it is tempting to speculate that changes upon reprogramming and epigenetic changes causing PHP1B are connected, the molecular mechanisms causing these changes are not identified. In contrast to our results in PSCs, loss of methylation at the AS DMR of *GNAS* is common in sporadic PHP1B (Maupetit-Méhouas et al., 2011) as observed for the A/B and XL DMRs, also methylated on the maternal allele). The mechanisms causing the epigenetic changes in PHP1B are under investigation and multiple. Some common mechanism might exist during reprogramming and PHP1B. Further studies analyzing the specific increase in AS methylation as well as the changes in other DMRs methylation observed in progenies from hESCs and hiPSCs may help understand the mechanisms whereby methylation at each DMR is controlled in physiology and the mechanisms leading to methylation defect in PHP1B.

The notion that loss of methylation at the *GNAS* DMRs controls transcript expression is mostly intuitive, with little available direct evidence. Freson et al. (2008) showed decreased methylation at XL DMR and increased expression of the XL protein in platelets. Loss of methylation at exon A/B is associated with an increase in the levels of the noncoding *exon A/B* RNA and a loss of *Gsα* expression (Bastepe and Jüppner 2005; Fröhlich et al., 2010). Studies in mice have shown that paternal deletion of the exon 1A region results in reversal of *Gsα* allelic silencing with biallelic expression of *Gsα* (Liu et al., 2000; Williamson et al., 2004). Monoallelic expression of *Gsα* has been reported in a few studies and mainly mouse studies (for reviews, see Bastepe and Jüppner, 2005; Hayward et al., 2001; Levine, 2012; Linglart et al., 2013; Mantovani et al., 2012; Plagge and Kelsey, 2006; Weinstein et al., 2007). Human tissues expressing paternal *Gsα* allelic silencing are not easily accessible, and the correlation between transcript expression and DMR methylation is rarely reported. Predominant maternal origin of transcription of *Gsα* in human thyroid gland and gonads has been reported (Mantovani et al., 2002).

Using the distinguishing parental single-nucleotide polymorphism rs7121, we correlated allelic expression and DMR methylation in hiPSCs and after differentiation for the three imprinted transcripts (*A/B*, *XLsα*, and *NESP55*) and also defined their parental expression as well as that of *Gsα*. Allelic expression of the maternally imprinted *A/B* transcripts varied as a function of the cell line. As indicated above, A/B DMR has a maternal-specific germline methylation. It is therefore expected that, in hiPSCs and progenies, the expression of the *A/B* transcripts originates predominantly from the paternal allele. This was observed in hiPSC clones and progenies derived from one fibroblast line, but not from the other. Importantly, however, we found that *A/B* transcript expression was correlated with the degree of methylation at the A/B DMR, indicating that allelic-silencing mechanism of *A/B* expression is methylation dependent.

Evidence from AD-PHP1B patients as well as mouse models indicates that the expression levels of the two transcripts, *exon A/B* and *Gsα*, are oppositely regulated in *cis* in imprinted tissues (Plagge and Kelsey 2006; Williamson et al., 2004). Absence of paternal *Gsα* transcript expression is attributed at least in part to the prevention of *Gsα* expression by the expressed *A/B* transcript. As expected, we detected biallelic expression of *Gsα* in all hiPSCs and fibroblasts, independently of A/B DMR methylation and transcription. Regarding the results in progenies, tissue-specific silencing of paternal *Gsα* has been described in brown fat cells (Williamson et al., 2004) of mesenchymal origin) and specific neurons (Chen et al., 2009); however, we do not observe *Gsα* allelic silencing in the MSC and NSC studied. The MSC and NSC analyzed here have not reached the differentiation status of brown fat cells and imprinted

neurons, likely explaining our results and supporting the requirement of "terminal" cell differentiation for *Gsα* allelic silencing to occur, as previously shown in the kidney (Turan et al., 2014; Zheng et al., 2001).

In most tissues, XL DMR has a maternal-specific germline methylation; thus, XL DMR methylation, absence of maternal *XLsα* transcription, and monoallelic paternal expression are expected in hiPSCs and progenies. Surprisingly, the paternally expressed imprinted *XLsα* transcript showed biallelic expression in all hiPSC clones from the two parental fibroblast lines but, as expected, monoallelic expression in all progenies (except one, also unstable for *A/B*). Intriguingly, this biallelic expression of *XLsα* in all hiPSC clones was observed in spite of a maintained XL DMR methylation and thus was independent of a change in allele-specific DNA methylation. This indicates that imprinting mechanism of *XLsα* transcript expression is not methylation dependent (at least mostly).

Correlation between allelic expression of imprinted genes including *NESP55* and methylation of identified DMR has been previously reported in hESCs (Adewumi et al., 2007; Kim et al., 2007; Rugg-Gunn et al., 2007). An association between the variability observed in inter-cell line allelic expression status and the DMR DNA methylation was present in one study (Kim et al., 2007), but not others in which monoallelic *NESP55* expression associated with maintenance in NESP DMR methylation in hESCs (Adewumi et al., 2007; Rugg-Gunn et al., 2007). We detected the maternally expressed imprinted transcript *NESP55* in three hiPSC samples. In contrast to *A/B* and *XLsα* transcripts, expression was monoallelic in these hiPSCs. This stability in the monoallelic expression of *NESP55* in hiPSCs raises the possibility that the process that maintains methylation at NESP DMR (or protect the unmethylated allele against aberrant methylation) might differ for NESP whose imprint is acquired postfertilization.

In summary, our studies indicate that (1) methylation at the *GNAS* locus DMRs is DMR and cell line specific, (2) methylation at the A/B DMR is correlated with *A/B* transcript expression, and (3) changes in allelic transcript expression can be independent of a change in allele-specific DNA methylation. The study of parental, reprogrammed, and differentiated cells should provide a model for studying the mechanisms controlling *GNAS* methylation, such as hydroxymethylation (Smallwood and Kelsey 2012); factors involved in transcript expression; and possibly mechanisms involved in the pathophysiology of PHP1B. This model will benefit from the possibility of differentiating PSCs in cell types in which *Gsα* is paternally silenced, such as BAT (Elabd et al., 2009) or proximal tubule (Montserrat et al., 2012) as shown for Angelman and Prader-Willi syndromes, two neurodevelopmental disorders of genomic imprinting (Chamberlain et al., 2010).

EXPERIMENTAL PROCEDURES

Cell Lines

Human Embryonic Stem Cells

Four hESC lines were studied (Table 1). The hESC line VUB01 (XY; passages 80–100) was derived at the Vrije Universiteit Brussels, H9 (XX; passages 50–60; WA09) by the WiCell Institute, and RC9 (XY; passages 20–40) by Roslin Cells. The hESC line SA01 (XY; passages 30–50) is distributed by Cellartis.

Induced Pluripotent Stem Cells

hiPSC lines were obtained by reprogramming of two fibroblast lines (IMR90 and GM04603) obtained from the Coriell Institute either by retroviral or episomal methods as previously reported (Mangeot et al., 2011; Yu et al., 2009). For IMR90 (XX), two clones were studied: one obtained by retroviral methods (i90_c01) and one by episomal methods (i90_c17). For GM04603 (XY), a polyclonal (iPSC04603_polyF) and a clonal (iPSC04603_c27) line were studied (Table 1).

Pluripotent Stem Cell Culture

All PSC lines except RC9 were maintained on a feeder layer of mitomycin-C-inactivated murine embryonic fibroblast cells in a humidified 5% CO2 incubator at 37°C, in KnockOut (KO)-Dulbecco's modified Eagle's medium supplemented with 20% KO serum replacement, 1 mM L-glutamine, 1% nonessential amino acids, 0.1 mM β-mercaptoethanol, and 10 ng/ml basic (b)fibroblast growth factor (FGF) (all from Invitrogen). RC9 was maintained on a feeder-free system composed of CellStart matrix and StemPro medium supplemented with 10 ng/ml basic (b)FGF (Invitrogen). Cultures were fed daily and manually passaged every 5–7 days. Quality control of the PSCs was performed as suggested by the International Stem Cell Banking Initiative (2009) and showed normal karyotypes and expression of stemness markers.

Differentiation

Differentiation of PSCs into mesenchymal (MSC) (hESC lines: W09; hiPSC: i90_c01, i90_c17, and 4603_c27) and neural (NSC) (hESC lines: SA01 and VUB01; hiPSC: i90_c17 and 4603_c27) progenies was performed as previously reported (Benchoua and Peschanski 2013; Chambers et al., 2009; Giraud-Triboult et al., 2011; Guenou et al., 2009) (Table 1).

DNA Extraction

Genomic DNA was extracted from parental fibroblasts, undifferentiated and differentiated PSC lines (except one, NSC i90c01; Table 1), and from peripheral blood mononuclear cells from 20 control subjects using Gentra Kit extraction (QIAGEN) according to the manufacturer's protocol. Informed written consent was obtained from the controls for genomic DNA (gDNA) analysis.

Quantification of DNA Methylation

Quantification of *GNAS* DMRs DNA methylation was performed by pyrosequencing as described in Supplemental Information and Maupetit-Méhouas et al. (2013). Six hundred nanograms of DNA were bisulfite converted (EZ DNA Methylation-Gold

Kit; Zymo Research) according to the manufacturer's protocol. One microliter of bisulfite-converted DNA was then amplified with specific primers for each DMR (A/B, XL, AS, and NESP). Pyrosequencing reactions were carried out on a PyroMark Q96 ID (QIAGEN) using either one sequencing primer for two distinct bisulfited PCR products (NESP, AS, and XL DMRs) or two different sequencing primers of one bisulfited PCR product (A/B DMR). Primer sequences and PCR conditions are presented in Table S1. The peak heights were determined using the provided software (PyroMark Q24 v2.0.6.20). Results are the mean ± SD of methylation measured at each cytosine for each DMR (NESP and XL 5 cytosines; AS: seven cytosines; A/B: eight cytosines). Replicate differences between <10% and 10% were considered inherent to the technique. In the rare cases of differences >10%, additional analysis pyrosequencing was performed. Five specific DNAs were included in each run and served as internal standards to ensure repeatability: unmethylated DNA (whole-genome amplified control DNA generated using the REPLI-g Mini Kit [QIAGEN]), fully methylated DNA (unmethylated DNA treated with SSI DNA methyltransferase [New England Biolabs]), one DNA prepared from a patient carrying an ~1.7 Mb 20q paternal deletion comprising the *GNAS* locus (I. Garin, F.M. Elli, A.L., C.S., L. de Sanctis, P. Bordogna, A. Pereda, J.T.R. Clarke, C. Kannengiesser, R. Coutant, Y. Tenebaum-Rakover, International Clinical Group for PHP, EuroPHP Consortium, G.P. de Nanclares, and G. Mantovani, unpublished data), one DNA obtained from a patient with paternal *GNAS* duplication (Maupetit-Méhouas et al., 2013), and one control DNA.

Complementary DNA

Total RNA were extracted from 1 × 10^6 frozen cells pellet using Trizol reagent (Invitrogen) followed by a treatment in the RNeasy MinElute cleanup Kit (QIAGEN) according to the manufacturer's protocol. Integrity of RNA was verified on 1.5% agarose gel electrophoresis. One microgram total RNA digested by DNaseI (Fermentas) was reverse transcribed using either hexamer random primers (for the transcript allelic expression analysis, see below) or oligo (dT) primers (for the quantitative real-time PCR, see below; RevertedAid H Minus First Strand cDNA synthesis Kit; Fermentas) according to the manufacturer's protocol.

GNAS rs7121 Polymorphism Analysis in Genomic and cDNA

For gDNA, 200 ng samples were PCR amplified with forward and reverse primers localized in introns 3 and 5, respectively, covering exons 4 and 6 of *GNAS* (exons common to *Gsα*, *XLsα*, *A/B*, and *NESP55*) (Table S2). In order to allow analysis of C and T allele ratio by bidirectional pyrosequencing (see below), two PCRs were performed for each product, with either the forward or reverse primer being biotinylated. DNA PCR products were checked by migration on 1.5% agarose gel electrophoresis.

For cDNA, 1 µl of cDNA was amplified with a forward-specific primer for *Gsα*, *XLsα*, *A/B*, and *NESP*55 transcripts, localized in their respective exon 1, and a reverse primer common of all transcripts except *GNAS-AS1* localized in exons 9 and 10 (Table S2). As for gDNA, two PCRs were performed for each product, with either the forward or reverse primer being biotinylated. cDNA PCR products were checked by migration on 1.5% agarose gel electrophoresis.

Heterozygosity at the *GNAS* Polymorphism rs7121 and Transcript Allelic Expression Analysis

C and T allele ratio was analyzed by bidirectional pyrosequencing using forward- and reverse-sequencing primers localized in exon 5 (Table S2) on PCR products obtained from gDNA and cDNA (described above). Ratios were calculated using the Pyrosequencing software. A similar approach has been reported (Klenke et al., 2011). DNA heterozygosity was defined for C (or T) allele ratio comprised between 40% and 60%.

Comparison of C or T allele ratio of cDNA samples were analyzed only from heterozygous gDNA samples for rs7121 (T393C). When detected, *NESP55* transcript expression was monoallelic (>94% C in clone hiPSC90_c01 and >94% T in clone hiPSC 4603_c27 and polyF) (Figure S3; Results). Given that in "physiological" conditions, *NESP55* is essentially maternally expressed, expression for *GNAS* transcripts is thus expressed as percent maternal allele ratio. Biallelic expression was defined for maternal allele ratio comprised between 40% and 60% and monoallelic expression for maternal allele ratio comprised between 90% and 100% and 0% and 10%. Examples of heterozygosity at the DNA level, biallelic (*Gsα*) and monoallelic (*NESP55*) transcript expressions quantified by pyrosequencing are shown on Figure S4.

Allelic expression was analyzed for parental IMR90 and GM04603 fibroblasts, all derived hiPSC (i90_c01, i90_c17, 4603_c27, and 4603_polyF), and for MSC (i90_c01, i90_c17, and 4603_c27) and neural (i90_c17 and 4603_c27) progenies (Table 1). Allelic expression was not studied in other samples either because the rs7121 polymorphism was present at the homozygous state (all hESCs) or no RNA was available.

Quantitative Real-Time PCR Analysis

Two qRT-PCR technologies were performed. The Sybr Green technology was used to detect *Gsα*, *A/B*, *XLsα*, *NESP55*, and glyceraldehyde 3-phosphate dehydrogenase (*GAPDH*) transcripts, and the Taqman technology was used to detect *GNAS-AS1*. Real-time PCR was carried out in a LightCycler LC480 system (Roche) to amplify *Gsα*, *A/B*, *XLsα*, *NESP55*, and *GAPDH* transcripts and an Applied Biosystems 7500 Fast Real-Time PCR System (Life Technologies) to amplify *GNAS-AS1*.

One microliter of cDNA (see above) was amplified using the LightCycler 480 SYBR Green I Master (Roche) for *Gsα*, *XLsα*, *NESP55*, and *GAPDH* transcripts, the Luminaris HiGreen qPCR Master Mix (Thermo Scientific) for *A/B* transcript, and the GoTaq Probe qPCR Master Mix (Promega) for *GNAS-AS1*. All PCR experiments were performed in triplicate. *GNAS-AS1* mRNA level was quantified using a commercially Taqman assay (Hs.PT.58.25851302; Integrated DNA Technologies). Specific pairs of primers were used to amplify other transcripts (Eurofins; primers and PCR conditions available upon request).

Specificity of amplified qRT-PCR products was verified by performing a melting curve analysis at the end of amplification (Sybr Green technology only) and by migration on 1.5% agarose gel electrophoresis. Gene expression was normalized with human *GAPDH* as endogenous gene control using the formula NE = $E_{reference}^{CTreference}/E_{target}^{CTtarget}$ (Simon 2003), where NE is the normalized expression, E the efficiency of the PCR amplification for the reference ($E_{reference}$) and the target (E_{target}), and CT the

threshold cycle of the transcript detection. Primers used for *Gsα* amplification were previously described (Mariot et al., 2011). PCR amplification efficiency was comprised between 1.85 and 1.97.

Statistical Analysis

Methylation indices (MI) DMR at each DMR and dispersion of MI were compared by Kruskal-Wallis test followed by Dunn's multiple comparison test. A p value < 0.05 was considered significant. To calculate the dispersion of MI, the mean of DMR MI for each group was calculated and the deviation of each sample to the mean calculated. Statistical analyses have been performed using Prism software.

SUPPLEMENTAL INFORMATION

Supplemental Information includes five figures and two tables and can be found with this article online at http://dx.doi.org/10.1016/j.stemcr.2014.07.002.

ACKNOWLEDGMENTS

This work was supported by recurrent INSERM funding. V.G. received a grant from the French Society of Pediatric Endocrinology and Diabetology.

Received: February 21, 2014
Revised: July 4, 2014
Accepted: July 7, 2014
Published: August 7, 2014

REFERENCES

Adewumi, O., Aflatoonian, B., Ahrlund-Richter, L., Amit, M., Andrews, P.W., Beighton, G., Bello, P.A., Benvenisty, N., Berry, L.S., Bevan, S., et al.; International Stem Cell Initiative (2007). Characterization of human embryonic stem cell lines by the International Stem Cell Initiative. Nat. Biotechnol. *25*, 803–816.

Bastepe, M., and Jüppner, H. (2005). GNAS locus and pseudohypoparathyroidism. Horm. Res. *63*, 65–74.

Benchoua, A., and Peschanski, M. (2013). Pluripotent stem cells as a model to study non-coding RNAs function in human neurogenesis. Front Cell Neurosci *7*, 140.

Chamberlain, S.J., Chen, P.F., Ng, K.Y., Bourgois-Rocha, F., Lemtiri-Chlieh, F., Levine, E.S., and Lalande, M. (2010). Induced pluripotent stem cell models of the genomic imprinting disorders Angelman and Prader-Willi syndromes. Proc. Natl. Acad. Sci. USA *107*, 17668–17673.

Chambers, S.M., Fasano, C.A., Papapetrou, E.P., Tomishima, M., Sadelain, M., and Studer, L. (2009). Highly efficient neural conversion of human ES and iPS cells by dual inhibition of SMAD signaling. Nat. Biotechnol. *27*, 275–280.

Chen, M., Wang, J., Dickerson, K.E., Kelleher, J., Xie, T., Gupta, D., Lai, E.W., Pacak, K., Gavrilova, O., and Weinstein, L.S. (2009). Central nervous system imprinting of the G protein G(s)alpha and its role in metabolic regulation. Cell Metab. *9*, 548–555.

Chotalia, M., Smallwood, S.A., Ruf, N., Dawson, C., Lucifero, D., Frontera, M., James, K., Dean, W., and Kelsey, G. (2009). Transcription is required for establishment of germline methylation marks at imprinted genes. Genes Dev. *23*, 105–117.

Coombes, C., Arnaud, P., Gordon, E., Dean, W., Coar, E.A., Williamson, C.M., Feil, R., Peters, J., and Kelsey, G. (2003). Epigenetic properties and identification of an imprint mark in the Nesp-Gnasxl domain of the mouse Gnas imprinted locus. Mol. Cell. Biol. *23*, 5475–5488.

Crane, J.L., Shamblott, M.J., Axelman, J., Hsu, S., Levine, M.A., and Germain-Lee, E.L. (2009). Imprinting status of Galpha(s), NESP55, and XLalphas in cell cultures derived from human embryonic germ cells: GNAS imprinting in human embryonic germ cells. Clin. Transl. Sci. *2*, 355–360.

Elabd, C., Chiellini, C., Carmona, M., Galitzky, J., Cochet, O., Petersen, R., Pénicaud, L., Kristiansen, K., Bouloumié, A., Casteilla, L., et al. (2009). Human multipotent adipose-derived stem cells differentiate into functional brown adipocytes. Stem Cells *27*, 2753–2760.

Freson, K., Izzi, B., Labarque, V., Van Helvoirt, M., Thys, C., Wittevrongel, C., Bex, M., Bouillon, R., Godefroid, N., Proesmans, W., et al. (2008). GNAS defects identified by stimulatory G protein alpha-subunit signalling studies in platelets. J. Clin. Endocrinol. Metab. *93*, 4851–4859.

Fröhlich, L.F., Mrakovcic, M., Steinborn, R., Chung, U.I., Bastepe, M., and Jüppner, H. (2010). Targeted deletion of the Nesp55 DMR defines another Gnas imprinting control region and provides a mouse model of autosomal dominant PHP-Ib. Proc. Natl. Acad. Sci. USA *107*, 9275–9280.

Frost, J., Monk, D., Moschidou, D., Guillot, P.V., Stanier, P., Minger, S.L., Fisk, N.M., Moore, H.D., and Moore, G.E. (2011). The effects of culture on genomic imprinting profiles in human embryonic and fetal mesenchymal stem cells. Epigenetics *6*, 52–62.

Girardot, M., Feil, R., and Llères, D. (2013). Epigenetic deregulation of genomic imprinting in humans: causal mechanisms and clinical implications. Epigenomics *5*, 715–728.

Giraud-Triboult, K., Rochon-Beaucourt, C., Nissan, X., Champon, B., Aubert, S., and Piétu, G. (2011). Combined mRNA and microRNA profiling reveals that miR-148a and miR-20b control human mesenchymal stem cell phenotype via EPAS1. Physiol. Genomics *43*, 77–86.

Gkountela, S., Li, Z., Vincent, J.J., Zhang, K.X., Chen, A., Pellegrini, M., and Clark, A.T. (2013). The ontogeny of cKIT+ human primordial germ cells proves to be a resource for human germ line reprogramming, imprint erasure and in vitro differentiation. Nat. Cell Biol. *15*, 113–122.

Guenou, H., Nissan, X., Larcher, F., Feteira, J., Lemaitre, G., Saidani, M., Del Rio, M., Barrault, C.C., Bernard, F.X., Peschanski, M., et al. (2009). Human embryonic stem-cell derivatives for full reconstruction of the pluristratified epidermis: a preclinical study. Lancet *374*, 1745–1753.

Hayward, B.E., Kamiya, M., Strain, L., Moran, V., Campbell, R., Hayashizaki, Y., and Bonthron, D.T. (1998a). The human GNAS1 gene is imprinted and encodes distinct paternally and biallelically expressed G proteins. Proc. Natl. Acad. Sci. USA *95*, 10038–10043.

Hayward, B.E., Moran, V., Strain, L., and Bonthron, D.T. (1998b). Bidirectional imprinting of a single gene: GNAS1 encodes

maternally, paternally, and biallelically derived proteins. Proc. Natl. Acad. Sci. USA *95*, 15475–15480.

Hayward, B.E., Barlier, A., Korbonits, M., Grossman, A.B., Jacquet, P., Enjalbert, A., and Bonthron, D.T. (2001). Imprinting of the G(s) alpha gene GNAS1 in the pathogenesis of acromegaly. J. Clin. Invest. *107*, R31–R36.

Huntriss, J., Woodfine, K., Huddleston, J.E., Murrell, A., Rutherford, A.J., Elder, K., Khan, A.A., Hemmings, K., and Picton, H. (2011). Quantitative analysis of DNA methylation of imprinted genes in single human blastocysts by pyrosequencing. Fertil. Steril. *95*, 2564–2567, e1–e8.

International Stem Cell Banking Initiative (2009). Consensus guidance for banking and supply of human embryonic stem cell lines for research purposes. Stem Cell Rev. *5*, 301–314.

Kim, K.P., Thurston, A., Mummery, C., Ward-van Oostwaard, D., Priddle, H., Allegrucci, C., Denning, C., and Young, L. (2007). Gene-specific vulnerability to imprinting variability in human embryonic stem cell lines. Genome Res. *17*, 1731–1742.

Klenke, S., Siffert, W., and Frey, U.H. (2011). A novel aspect of GNAS imprinting: higher maternal expression of Gαs in human lymphoblasts, peripheral blood mononuclear cells, mammary adipose tissue, and heart. Mol. Cell. Endocrinol. *341*, 63–70.

Laird, D.J. (2013). Humans put their eggs in more than one basket. Nat. Cell Biol. *15*, 13–15.

Levine, M.A. (2012). An update on the clinical and molecular characteristics of pseudohypoparathyroidism. Curr. Opin. Endocrinol. Diabetes Obes. *19*, 443–451.

Li, Y., and Sasaki, H. (2011). Genomic imprinting in mammals: its life cycle, molecular mechanisms and reprogramming. Cell Res. *21*, 466–473.

Linglart, A., Maupetit-Méhouas, S., and Silve, C. (2013). GNAS-related loss-of-function disorders and the role of imprinting. Horm Res Paediatr *79*, 119–129.

Lister, R., Pelizzola, M., Kida, Y.S., Hawkins, R.D., Nery, J.R., Hon, G., Antosiewicz-Bourget, J., O'Malley, R., Castanon, R., Klugman, S., et al. (2011). Hotspots of aberrant epigenomic reprogramming in human induced pluripotent stem cells. Nature *471*, 68–73.

Liu, J., Yu, S., Litman, D., Chen, W., and Weinstein, L.S. (2000). Identification of a methylation imprint mark within the mouse Gnas locus. Mol. Cell. Biol. *20*, 5808–5817.

Lund, R.J., Närvä, E., and Lahesmaa, R. (2012). Genetic and epigenetic stability of human pluripotent stem cells. Nat. Rev. Genet. *13*, 732–744.

MacDonald, W.A., and Mann, M.R. (2014). Epigenetic regulation of genomic imprinting from germ line to preimplantation. Mol. Reprod. Dev. *81*, 126–140.

Mangeot, P.E., Dollet, S., Girard, M., Ciancia, C., Joly, S., Peschanski, M., and Lotteau, V. (2011). Protein transfer into human cells by VSV-G-induced nanovesicles. Mol. Ther. *19*, 1656–1666.

Mantovani, G., Ballare, E., Giammona, E., Beck-Peccoz, P., and Spada, A. (2002). The gsalpha gene: predominant maternal origin of transcription in human thyroid gland and gonads. J. Clin. Endocrinol. Metab. *87*, 4736–4740.

Mantovani, G., Elli, F.M., and Spada, A. (2012). GNAS epigenetic defects and pseudohypoparathyroidism: time for a new classification? Horm. Metab. Res. *44*, 716–723.

Mariot, V., Wu, J.Y., Aydin, C., Mantovani, G., Mahon, M.J., Linglart, A., and Bastepe, M. (2011). Potent constitutive cyclic AMP-generating activity of XLαs implicates this imprinted GNAS product in the pathogenesis of McCune-Albright syndrome and fibrous dysplasia of bone. Bone *48*, 312–320.

Maupetit-Méhouas, S., Mariot, V., Reynès, C., Bertrand, G., Feillet, F., Carel, J.C., Simon, D., Bihan, H., Gajdos, V., Devouge, E., et al. (2011). Quantification of the methylation at the GNAS locus identifies subtypes of sporadic pseudohypoparathyroidism type Ib. J. Med. Genet. *48*, 55–63.

Maupetit-Méhouas, S., Azzi, S., Steunou, V., Sakakini, N., Silve, C., Reynes, C., Perez de Nanclares, G., Keren, B., Chantot, S., Barlier, A., et al. (2013). Simultaneous hyper- and hypomethylation at imprinted loci in a subset of patients with GNAS epimutations underlies a complex and different mechanism of multilocus methylation defect in pseudohypoparathyroidism type 1b. Hum. Mutat. *34*, 1172–1180.

Montserrat, N., Ramírez-Bajo, M.J., Xia, Y., Sancho-Martinez, I., Moya-Rull, D., Miquel-Serra, L., Yang, S., Nivet, E., Cortina, C., González, F., et al. (2012). Generation of induced pluripotent stem cells from human renal proximal tubular cells with only two transcription factors, OCT4 and SOX2. J. Biol. Chem. *287*, 24131–24138.

Nazor, K.L., Altun, G., Lynch, C., Tran, H., Harness, J.V., Slavin, I., Garitaonandia, I., Müller, F.J., Wang, Y.C., Boscolo, F.S., et al. (2012). Recurrent variations in DNA methylation in human pluripotent stem cells and their differentiated derivatives. Cell Stem Cell *10*, 620–634.

Plagge, A., and Kelsey, G. (2006). Imprinting the Gnas locus. Cytogenet. Genome Res. *113*, 178–187.

Reik, W., Dean, W., and Walter, J. (2001). Epigenetic reprogramming in mammalian development. Science *293*, 1089–1093.

Rugg-Gunn, P.J., Ferguson-Smith, A.C., and Pedersen, R.A. (2005a). Epigenetic status of human embryonic stem cells. Nat. Genet. *37*, 585–587.

Rugg-Gunn, P.J., Ferguson-Smith, A.C., and Pedersen, R.A. (2005b). Human embryonic stem cells as a model for studying epigenetic regulation during early development. Cell Cycle *4*, 1323–1326.

Rugg-Gunn, P.J., Ferguson-Smith, A.C., and Pedersen, R.A. (2007). Status of genomic imprinting in human embryonic stem cells as revealed by a large cohort of independently derived and maintained lines. Hum. Mol. Genet. *16 Spec No. 2*, R243–R251.

Sabour, D., and Schöler, H.R. (2012). Reprogramming and the mammalian germline: the Weismann barrier revisited. Curr. Opin. Cell Biol. *24*, 716–723.

Simon, P. (2003). Q-Gene: processing quantitative real-time RT-PCR data. Bioinformatics *19*, 1439–1440.

Smallwood, S.A., and Kelsey, G. (2012). De novo DNA methylation: a germ cell perspective. Trends Genet. *28*, 33–42.

Takikawa, S., Ray, C., Wang, X., Shamis, Y., Wu, T.Y., and Li, X. (2013). Genomic imprinting is variably lost during reprogramming of mouse iPS cells. Stem Cell Res. (Amst.) *11*, 861–873.

Tobin, S.C., and Kim, K. (2012). Generating pluripotent stem cells: differential epigenetic changes during cellular reprogramming. FEBS Lett. *586*, 2874–2881.

Turan, S., Fernandez-Rebollo, E., Aydin, C., Zoto, T., Reyes, M., Bounoutas, G., Chen, M., Weinstein, L.S., Erben, R.G., Marshansky, V., and Bastepe, M. (2014). Postnatal establishment of allelic Gαs silencing as a plausible explanation for delayed onset of parathyroid hormone resistance owing to heterozygous Gαs disruption. J. Bone Miner. Res. *29*, 749–760.

Weinstein, L.S., Yu, S., Warner, D.R., and Liu, J. (2001). Endocrine manifestations of stimulatory G protein alpha-subunit mutations and the role of genomic imprinting. Endocr. Rev. *22*, 675–705.

Weinstein, L.S., Xie, T., Zhang, Q.H., and Chen, M. (2007). Studies of the regulation and function of the Gs alpha gene Gnas using gene targeting technology. Pharmacol. Ther. *115*, 271–291.

Williamson, C.M., Ball, S.T., Nottingham, W.T., Skinner, J.A., Plagge, A., Turner, M.D., Powles, N., Hough, T., Papworth, D., Fraser, W.D., et al. (2004). Acis-acting control region is required exclusively for the tissue-specific imprinting of Gnas. Nat. Genet. *36*, 894–899.

Yu, J., Hu, K., Smuga-Otto, K., Tian, S., Stewart, R., Slukvin, I.I., and Thomson, J.A. (2009). Human induced pluripotent stem cells free of vector and transgene sequences. Science *324*, 797–801.

Zheng, H., Radeva, G., McCann, J.A., Hendy, G.N., and Goodyer, C.G. (2001). Galphas transcripts are biallelically expressed in the human kidney cortex: implications for pseudohypoparathyroidism type 1b. J. Clin. Endocrinol. Metab. *86*, 4627–4629.